Article

Experimental Thermal Conductivity Studies of Agar-Based Aqueous Suspensions with Lignin Magnetic Nanocomposites

Bishal Gautam [1,†], **Saja M. Nabat Al-Ajrash** [1,†], **Mohammad Jahid Hasan** [2], **Abhishek Saini** [3], **Sarah J. Watzman** [3], **Esteban Ureña-Benavides** [2] **and Erick S. Vasquez-Guardado** [1,*]

1 Department of Chemical and Materials Engineering, University of Dayton, 300 College Park Ave., Dayton, OH 45469, USA; gautamb1@udayton.edu (B.G.); sajamodher0@gmail.com (S.M.N.A.-A.)
2 Department of Biomedical Engineering and Chemical Engineering, The University of Texas at San Antonio, One UTSA Circle, San Antonio, TX 78249, USA; mohammadjahid.hasan@utsa.edu (M.J.H.); esteban.urena-benavides@utsa.edu (E.U.-B.)
3 Department of Mechanical and Materials Engineering, University of Cincinnati, 2901 Woodside Drive, Cincinnati, OH 45221, USA; sainiak@mail.uc.edu (A.S.); watzmasj@ucmail.uc.edu (S.J.W.)
* Correspondence: evasquez1@udayton.edu; Tel.: +1-(937)-229-2627
† These authors contributed equally to this work.

Abstract: Nanoparticle additives increase the thermal conductivity of conventional heat transfer fluids at low concentrations, which leads to improved heat transfer fluids and processes. This study investigates lignin-coated magnetic nanocomposites (lignin@Fe_3O_4) as a novel bio-based magnetic nanoparticle additive to enhance the thermal conductivity of aqueous-based fluids. Kraft lignin was used to encapsulate the Fe_3O_4 nanoparticles to prevent agglomeration and oxidation of the magnetic nanoparticles. Lignin@Fe_3O_4 nanoparticles were prepared using a pH-driven co-precipitation method with a 3:1 lignin to magnetite ratio and characterized by X-ray diffraction, FT-IR, thermogravimetric analysis, and transmission electron microscopy. The magnetic properties were characterized using a vibrating sample magnetometer. Once fully characterized, lignin@Fe_3O_4 nanoparticles were dispersed in aqueous 0.1% w/v agar–water solutions at five different concentrations, from 0.001% w/v to 0.005% w/v. Thermal conductivity measurements were performed using the transient line heat source method at various temperatures. A maximum enhancement of 10% in thermal conductivity was achieved after adding 0.005% w/v lignin@Fe_3O_4 to the agar-based aqueous suspension at 45 °C. At room temperature (25 °C), the thermal conductivity of lignin@Fe_3O_4 and uncoated Fe_3O_4 agar-based suspensions was characterized at varying magnetic fields from 0 to 0.04 T, which were generated using a permanent magnet. For this analysis, the thermal conductivity of lignin magnetic nanosuspensions initially increased, showing a 5% maximum peak increase after applying a 0.02 T magnetic field, followed by a decreasing thermal conductivity at higher magnetic fields up to 0.04 T. This result is attributed to induced magnetic nanoparticle aggregation under external applied magnetic fields. Overall, this work demonstrates that lignin-coated Fe_3O_4 nanosuspension at low concentrations slightly increases the thermal conductivity of agar aqueous-based solutions, using a simple permanent magnet at room temperature or by adjusting temperature without any externally applied magnetic field.

Keywords: lignin@Fe_3O_4; lignin nanocomposites; thermal conductivity measurements; magnetic nanoparticles; lignin; transient line heat source method

1. Introduction

Heat transfer is a crucial phenomenon encountered in many devices, such as power generators, solar thermal systems, high-energy laser optics, electronic cooling devices, and heat exchangers [1,2]. Enhancing the thermal performance of such systems is crucial from an energy-saving perspective, which could be achieved by improving the thermal conductivity of conventional heat transfer fluids used on a larger industrial scale [1–5]. Over

the past three decades, several studies have approached this effort by dispersing metallic nanoparticles in fluids, demonstrating an increase in thermal conductivity compared to the carrier fluid [6,7]. Examples of such nanoparticle types include Fe_3O_4, silver oxide, and gold nanoparticles. In addition, the surface-to-volume ratio of nanoparticles potentially boosts contact with the fluid, reflecting enhanced thermal properties [8,9].

Experimental studies coupled with theoretical analyses, mathematical models, and computer simulations help to explain possible enhancement mechanisms or the abnormal behavior observed for the thermal conductivity of nanofluids [10]. For instance, Maxwell's classical model considered a dilute spherical particle suspension to increase thermal conductivity while ignoring the interactions among the particles [2]. Conversely, the dynamic model considers magnetic nanoparticles' random motion leading to the macromixing effect. This model concluded that the Brownian motion of the particles due to micromixing, clustering under a magnetic field, and improved heat conduction are the common mechanisms that enhance the fluid thermal conductivity [10]. Among metallic nanoparticles suspended in fluids, ferrofluids have unique features due to the ability to tailor the thermomagnetic convection by altering the carrier fluid properties, magnetic field, and temperature [11]. In addition, iron oxide has unique features such as biocompatibility, biodegradability, and superparamagnetic properties since these are used in many biomedical, environmental, and engineering applications [12]. It is one of the few nanoparticles the FDA has approved for research in cancer drug delivery, the water purification process, and many other industries to build an energy-efficient device [13,14]. Magnetite nanoparticles (Fe_3O_4) are of great interest due to technological applications in high-density magnetic recording media, catalysts, and clinical uses due to their superparamagnetic properties, higher adsorption ability, and surface functionalization capabilities [15]. Due to these unique characteristics, Fe_3O_4 nanoparticle-based nanocomposites are used to increase the thermal conductivity of traditional fluids. However, although Fe_3O_4 nanoparticles have appealing characteristics, such particles tend to aggregate more due to the strong van der Waals interaction between the particles [15,16]. Coating nanoparticles using various polymeric or biological materials is one of the potential solutions to prevent aggregation. Many studies have been performed using these Fe_3O_4-based nanocomposites on the requirements in biomedical research and clinical use [17]. These nanocomposites can change the magnetic behavior, pH, and stability within the suspension, which ultimately increases the thermal conductivity of colloidal nanosuspension in the presence of the magnetic field [18].

Lignin is a common sustainable polymeric material that could be utilized to fabricate sustainable nanocomposites. Among lignin, Kraft lignin is a natural heterogeneous polymer that accounts for 15–30% of the total plant biomass. The structural analysis of Kraft lignin provides evidence of a higher number of phenolic groups, which helps protect Fe_3O_4 nanoparticles against agglomeration and oxidation [19]. In addition, Kraft lignin contains aliphatic thiol and a higher amount of sulfur content, which helps create a hydrophobic nature of the lignin [20]. Due to the presence of aromatic rings with hydroxyl and methoxy functional groups, the oxidation propagation reaction can be terminated through hydrogen donation, resulting in the antioxidant properties of the lignin [20]. It is highly attractive as a ligand coating due to its hydrophobic nature, antioxidant properties, low cost of synthesis, and low toxicity. Lignin-based hybrid magnetic nanocomposites have exhibited a better adsorption rate using an external magnetic field due to good superparamagnetic properties [18,21]. Due to higher magnetic properties and a higher dispersion rate, lignin-based Fe_3O_4 nanocomposites are suitable agents that could enhance the thermal conductivity of traditional heat transfer fluids under different conditions [17,18,21].

Measuring the thermal conductivity of the low-viscosity fluids and aqueous suspensions at different temperatures presents significant challenges and limitations due to free convective heat transfer, e.g., particle settling over time makes the fluid unstable. Using more viscous carrying fluids such as agar stabilizes the particles and prevents them from settling, enabling thermal conductivity measurements. For example, Ebrahimi et al. [22] compared the accuracy of thermal conductivity measurements of water and an ethylene gly-

col/water solution stabilized by agar at different concentrations. The prepared nanofluid with agar showed high accuracy (within $\pm 2\%$ of those predicted by the Maxwell model). Hence, selecting the carrier fluid when the thermal conductivity properties of nanocomposite suspensions are measured is a critical aspect that needs to be considered.

In addition to selecting the nanoparticle type, the carrier fluid, and the nanoparticle concentration, the stabilizing coating or surfactant plays a important role in the nanocomposite's capability to enhance the thermal conductivity of a suspension. For example, magnetic nanosuspensions of Fe_3O_4 dispersed in a tetramethyl ammonium hydroxide solution have shown a maximum 11.5% thermal conductivity enhancement at 313.15 K and a 3 vol % concentration [23]. Recently, Sahu et al. reported the effect of using multiple surfactants for the stabilization of Fe_3O_4 nanoparticles on heating potentials [24]. Their results showed that the heating efficacy varied based on the different coatings, proving potential for clinical applications. Ternary magnetic nanocomposites comprised of reduced graphene, titanium dioxide, and Fe_3O_4, showed thermal conductivity enhancements of up to 13.3% at 333.15 K [25]. Polymers are also attractive coating materials for inorganic nanoparticles, which generate nanocomposites with enhanced thermal conductivity capable of performing as thermal interface materials for thermal management applications [26]. Bimetallic iron nanocomposites have also shown enhanced magnetic characteristics at different temperatures [27]. However, to our knowledge, there is a lack of thermal conductivity studies of bio-based polymer nanocomposites, including lignin@Fe_3O_4.

This experimental study seeks to obtain a better understanding of the effective thermal conductivity enhancement of agar-based aqueous suspensions using magnetite nanoparticles with and without lignin functionalization. Both magnetic nanoparticle types were dispersed in agar-based aqueous solutions to avoid convective effects, generally observed in water, to optimize the thermal conductivity measurements. Additionally, previous studies highlight the importance of using permanent magnets to tune the magnetic response of aqueous suspensions, including a low-cost magnetic field generation without a continuous energy supply [28] and enhanced pollutant adsorption removal rates from aqueous solutions [29]. Hence we also seek to better understand thermal conductivity measurements using rare Earth permanent magnets. In this study, the thermal conductivity of aqueous lignin@Fe_3O_4 agar-based suspensions are studied as a function of concentration, external magnetic field, or temperature. We discuss aspects related to the stability of the colloidal suspension under non-uniform magnetic fields generated when exposing the suspension to permanent magnets and their effect on the thermal conductivity measurements at room temperature. Thermal conductivity result comparisons between lignin@Fe_3O_4 nanoparticles and uncoated Fe_3O_4 nanoparticles are also analyzed under no externally applied magnetic fields for five concentrations at five different temperature conditions.

2. Materials and Methods

2.1. Materials

Kraft lignin (95% purity, 5% moisture) and ammonium hydroxide solution (28–30%) were supplied by Sigma-Aldrich (St. Louis, MO, USA). Ultra-pure type I water (EMD water purification system) and ACROS organics pure agar (99% pure) were used as received without any further purification. To synthesize the Fe_3O_4 nanoparticles, 98% iron (II) chloride and iron (III) chloride were utilized. A sonication bath (Branson 5800, Marshall Scientific, Hampton, NH, USA), a high-shear mixer (Turrax T-25, Cole-Parmer, Vernon Hills, IL, USA), and an overhead stirrer (IKA RW 20, Delft, The Netherlands) were used to stir and homogenize the colloidal suspensions.

In this study, Fe_3O_4 nanoparticles were synthesized using the co-precipitation method similar to Massart's procedure [30], Petrie's procedure [31], and Westphal's procedure [32]. The Fe_3O_4 nanoparticles were encapsulated with Kraft lignin solubilized in 1 wt% ammonium hydroxide to produce a 3:1 w:w ratio of lignin@Fe_3O_4 nanoparticles. The detailed procedure to synthesize lignin@Fe_3O_4 nanoparticles has been reported in

our previous publications [33–35], and a summary of the procedure can be found in the supplementary materials.

Lignin@Fe$_3$O$_4$ and Fe$_3$O$_4$ nanopowders were dispersed in 0.1% *w/v* aqueous agar solutions at a concentration of 0.001% *w/v*, 0.002% *w/v*, 0.003% *w/v*, 0.004% *w/v*, and 0.005% *w/v*, respectively (Figures 1 and 2). The colloidal suspensions were sonicated in a sonication bath for 4 h for complete dispersion. After 4 h of sonication, an ultrasonication homogenizer was used for 10 min for every sample for complete dispersion. The overhead stirrer was used for 5 min for every sample to mix the agar and nanoparticles solution.
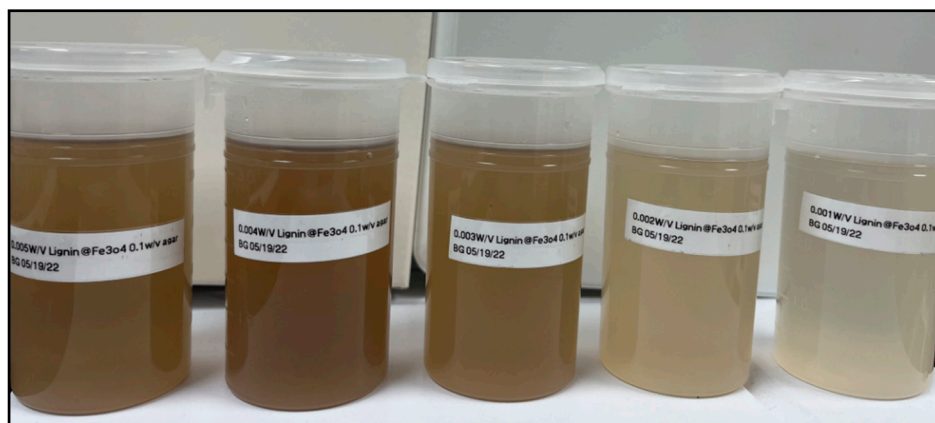
Figure 1. lignin@Fe$_3$O$_4$ suspended at various concentrations: 0.005% *w/v*, 0.004% *w/v*, 0.003% *w/v*, 0.002% *w/v*, and 0.001% *w/v*, (left-to right) in 0.1% *w/v* aqueous agar solution.
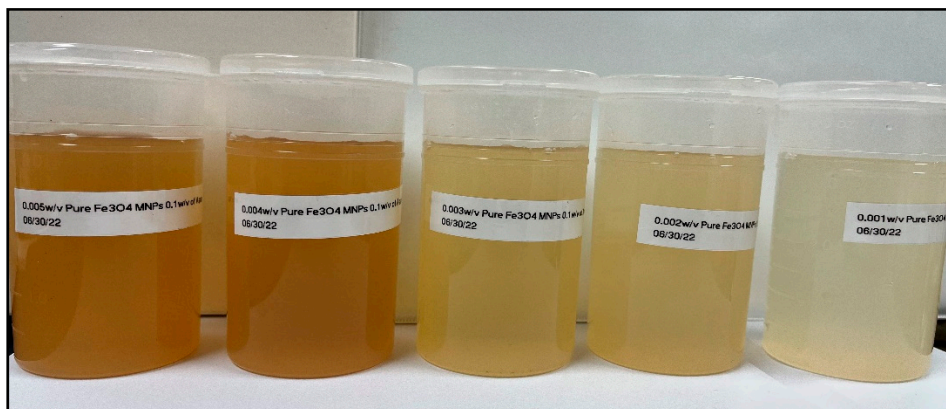

Figure 2. Visual inspection of uncoated Fe$_3$O$_4$ nanosuspension at a concentration of 0.005% *w/v*, 0.004% *w/v*, 0.003% *w/v*, 0.002% *w/v*, and 0.001% *w/v* (left-to-right) in 0.1% *w/v* aqueous agar solution.

2.2. Characterization Techniques

Various techniques were utilized to analyze the synthesized lignin@Fe$_3$O$_4$ nanoparticles and pure Fe$_3$O$_4$ nanoparticles. Fourier transform infrared spectroscopy (FT-IR) (Nicolet iS550 Spectrometer, Thermo Fisher Scientific, Waltham, MA, USA) was used to obtain the chemical structure of lignin@Fe$_3$O$_4$ nanoparticles. Thermogravimetric analysis (TGA, Q500, TA instruments, New Castle, DE, USA) was used to determine the thermal stability of the nanoparticles and the percentage of lignin encapsulation at the Fe$_3$O$_4$ nanoparticles' surface. The thermal analysis procedure consisted of a temperature ramp from ambient temperature (~22 °C) to 800 °C at a ramp rate of 10 °C/min under constant nitrogen flow in the sample chamber (90 mL/min).

The microscopic images of the lignin@Fe$_3$O$_4$ and uncoated Fe$_3$O$_4$ nanoparticles were obtained using a JEOL JEM-2010F High-resolution Transmission Electron Microscope (Nanolab technology, Milpitas, CA, USA). A dilute suspension of the samples (0.0002 wt%) was prepared. Then, one drop of each sample was placed on one Lacey Carbon 300-mesh

copper TEM grid and dried overnight. The dried TEM grids were then placed in the microscope and the images were obtained. X-ray diffraction (XRD) and Rigaku Smart XRD (Tokyo, Japan) with 40 kV voltage and 44 mA current identified the nanoparticles' crystalline structure. The magnetic properties of the particles were characterized using a Quantum Design Physical Property Measurement System (PPMS; San Diego, CA, USA) with a Vibrating Sample Magnetometer (VSM) option. Each powdered sample was loaded in a Quantum Design powder sample holder, and the loaded sample holder was snapped in a brass half-tube sample holder for each magnetization measurement. The magnetic moment of each of the two powdered samples was measured from −4 T to 4 T at 300 K. Additionally, temperature-dependent magnetization measurements were collected at 0.1 T (1000 Oe) from 2 to 300 K.

The thermal conductivity of the colloidal suspensions was measured using a TEMPOS thermal properties analyzer equipment (METER group's device, Pulman, WA, USA) with a KS-3 sensor probe, which uses the transient line heat source method. It has a probe consisting of a needle with a heater and temperature sensor inside. The system monitors the sensor's temperature when a current passes through the heater. Cole Parmer's water bath (Staffordshire, UK) was utilized to keep the sample at the desired temperature of 25 °C, 30 °C, 35 °C, 40 °C, and 45 °C, respectively. Each suspension was poured inside the sample holder and kept inside the water bath for 4 h for uniform temperature distribution throughout the sample, which was measured using a thermocouple. A KS-3 probe was used to measure the thermal conductivity of the nanosuspension. Each suspension was analyzed at the five different stabilized temperature conditions previously mentioned under no externally applied magnetic field. The schematic diagram to measure the thermal conductivity of the aqueous nanosuspensions is shown in Figure 3.
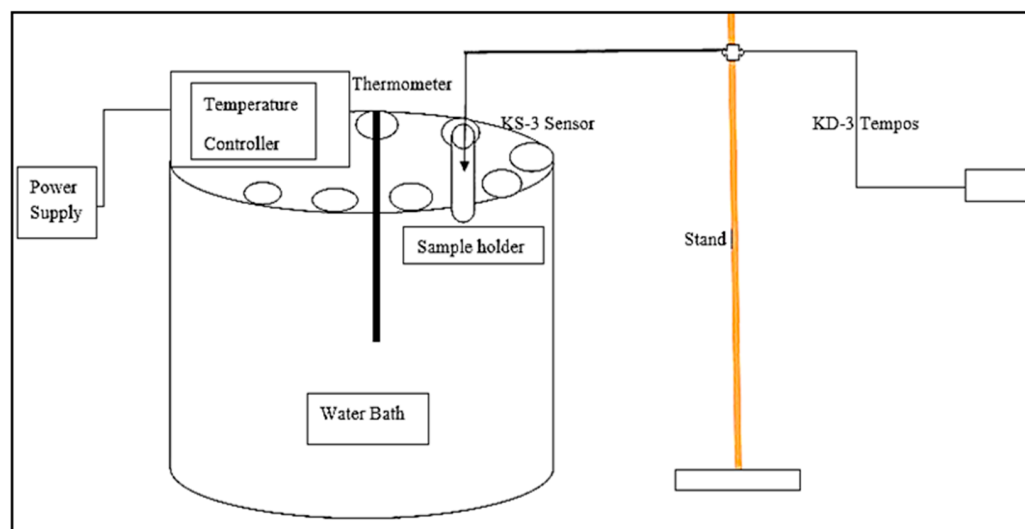

Figure 3. Schematic diagram showing the experimental procedure to measure the thermal conductivity of aqueous agar-based magnetic suspensions.

To measure magnetic field-dependent thermal conductivity measurements of the colloidal suspensions at room temperature (~22 °C), a neodymium magnet with a maximum field strength of 550 mT was utilized. Using a magnetic meter (PCE-MFM 3000 AC/DC, PCE Instruments, Jupiter, FL, USA) and prior to any thermal conductivity measurements, the magnetic field strength was measured at the center of the flask as the neodymium magnet was placed at different distances. Table S1 (Supplemental Information) shows the measured magnetic field strengths at different distances. After this calibration, each the suspension was placed in a 50 mL flask, with a 24/40 adapter holder at a known distance from the magnet, and the KS-3 probe was used to measure the thermal conductivity of each suspension. Note that all thermal conductivity measurements were conducted at room

temperature to avoid potential issues with temperature sensors. Full system calibration is suggested for future studies where temperature and externally induced magnetic fields are applied. A photograph of the setup utilized can be seen in Figure S1.

3. Results and Discussion

3.1. Morphological Characterization: Transmission Electron Microscopy (TEM)

Lacey carbon TEM grids were used to prepare the Fe_3O_4 and lignin@Fe_3O_4 nanoparticle samples. Figure 4A–C shows the dispersed nanoparticles, indicating the lignin encapsulation at the surface of the nanoparticles. Lighter regions are observed surrounding the magnetic core (Figure 4C), confirming the presence of lignin. Although the lignin coating does not entirely cover the iron oxide core, dispersion of lignin@Fe_3O_4 was achieved. For comparison purposes, uncoated Fe_3O_4 formed larger aggregated structures (Figure 4D,E). Previous studies have confirmed that the higher the ratio of lignin in the nanoparticles, the better they are dispersed in the solution. This is because of the dispersant nature of lignin in many industrial and laboratory-scale applications [31,36]. Recently, we demonstrated the adsorptive and magnetic response of lignin:Fe_3O_4 at a mass ratio of 3:1 [33]. Hence, we used the same ratio for analyzing the thermal conductivity enhancement caused by introducing lignin@Fe_3O_4 into agar-based suspensions in this study.
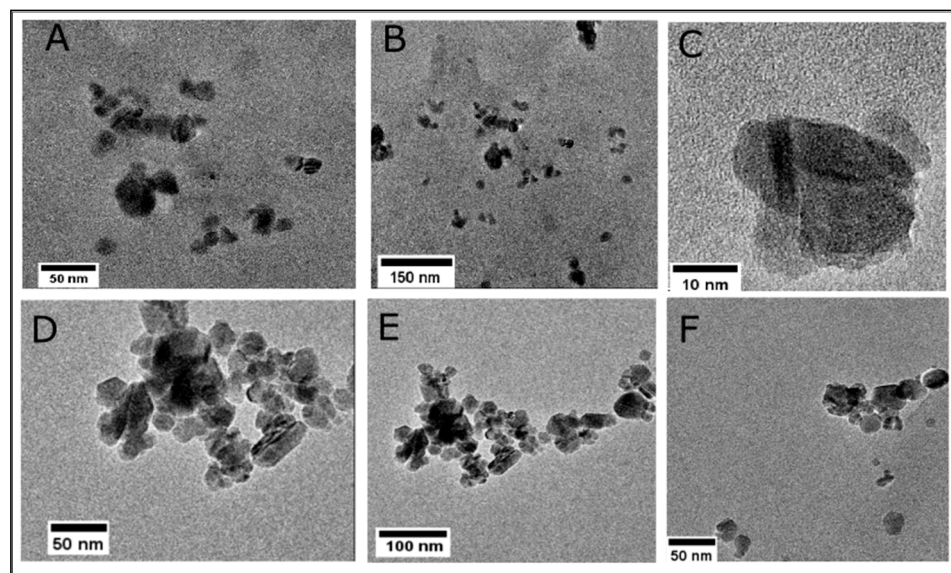

Figure 4. TEM images for a 3:1 mass ratio preparation of lignin@Fe_3O_4 nanoparticles (**A–C**) indicate the encapsulation of lignin at the surface of Fe_3O_4 nanoparticles. (**D–F**) show uncoated clusters of Fe_3O_4 nanoparticles. The lignin encapsulation avoids aggregation of the Fe_3O_4 nanoparticles.

3.2. Thermogravimetric Analysis (TGA) and Magnetization Properties

From the TGA curves (Figure 5), it is noted that neat Kraft lignin lost almost 61.88% of its original mass at ~800 °C, with the initial decomposition starting at ~200 °C. Furthermore, a rapid weight loss of ~45% for Kraft lignin was observed at temperatures between 100 °C and 400 °C. Below 100 °C, the TGA results confirmed water evaporation initially present in the as-received lignin. On the contrary, uncoated Fe_3O_4 only lost 0.84% solid content within the same temperature heating range. This result confirms the high thermal stability of the untreated magnetic nanoparticle. The lignin@Fe_3O_4 nanocomposites, on the other hand, lost 11%, indicating a 16.6 wt.% loading of lignin coating onto the magnetic nanoparticles' surfaces. Most of the weight loss of lignin@Fe_3O_4 occurred between 300 °C and 700 °C, where the lignin decomposition occurs (Figure 5), confirming the presence of lignin in the nanocomposite.
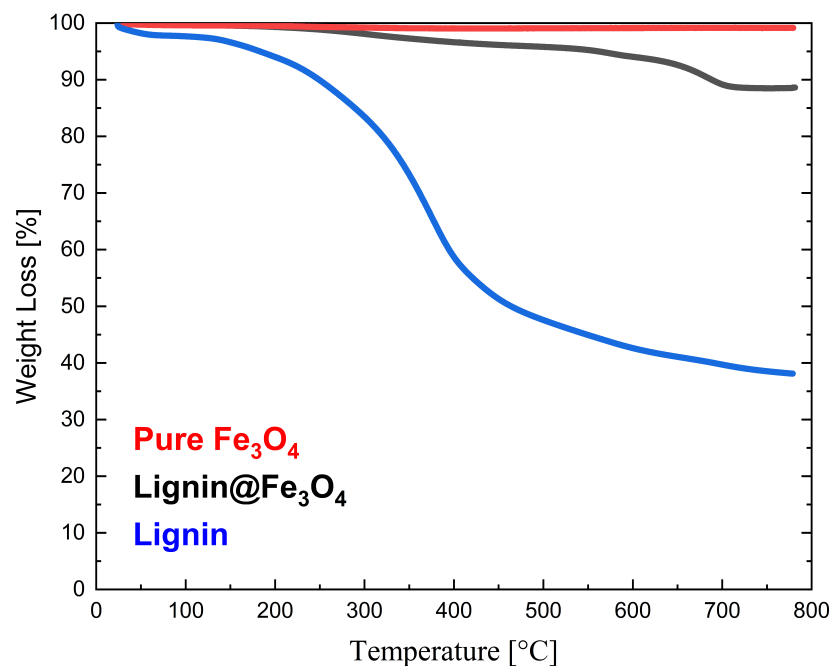
Figure 5. Thermogravimetric analysis (TGA) of Kraft lignin, Fe_3O_4, and lignin@Fe_3O_4.

The magnetization measurement results determined via VSM at 300 K (~27 °C) are shown in Figure 6. The VSM measurement was normalized with the weight of the measured sample. The results showed that pure Fe_3O_4 nanoparticles have slightly higher saturation magnetization (M_s) than lignin@Fe_3O_4 nanoparticles. Lignin-coated Fe_3O_4 showed an M_s of 74 emu/g, whereas pure Fe_3O_4 had an M_s of 76 emu/g. The slight M_s difference is attributed to the Fe_3O_4 content. Additional information about the magnetic properties of the lignin@Fe_3O_4 nanocomposite compared with the uncoated Fe_3O_4 was obtained through magnetization–temperature profile measurement using the same VSM system (Figure 7).
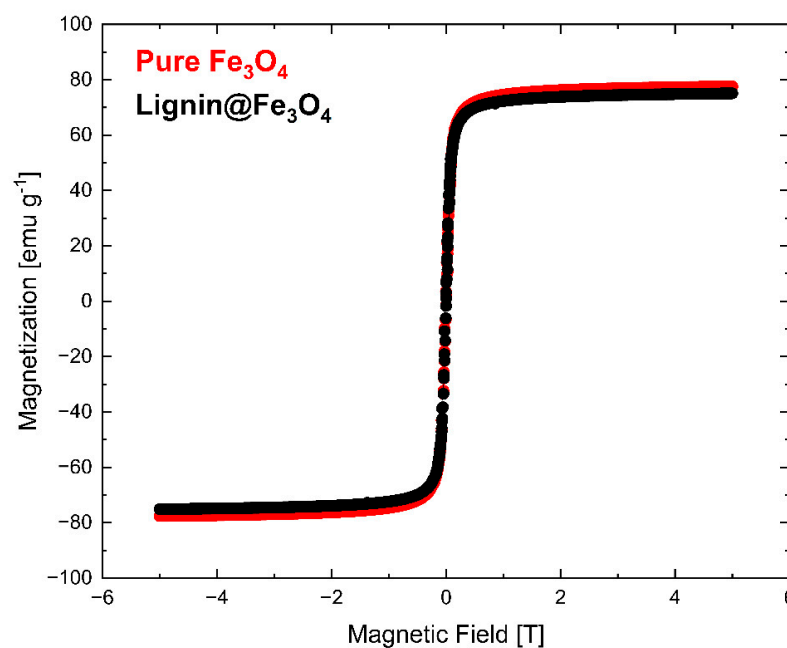

Figure 6. Magnetization measurement results (VSM) show the saturation magnetization of pure Fe_3O_4 and lignin@Fe_3O_4 at 300 K.
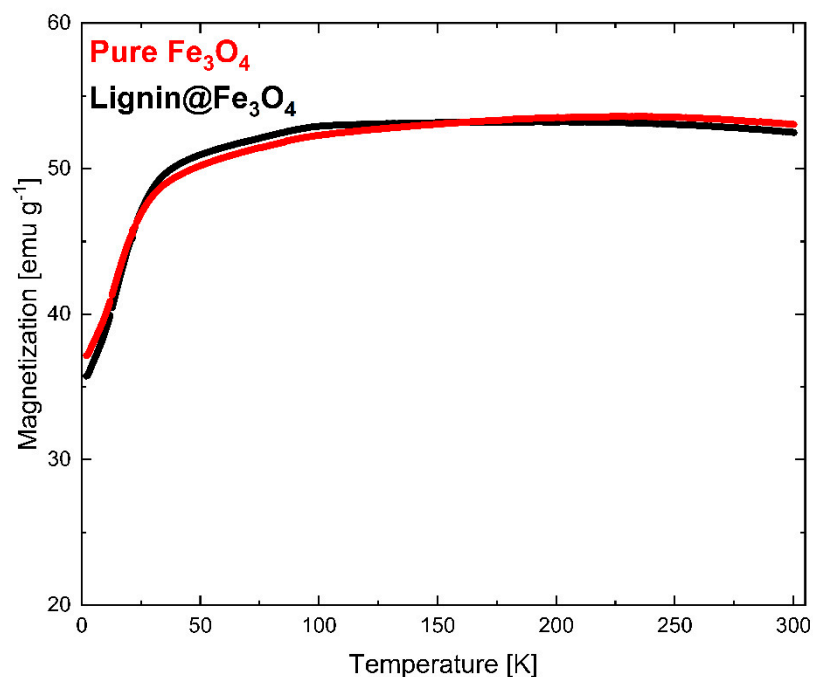
Figure 7. Magnetization vs. temperature profiles for Fe_3O_4 and lignin@Fe_3O_4 under a 0.1 T externally applied magnetic field.

The magnetization curves at 300 K showed that pure Fe_3O_4 nanoparticles have a slightly higher magnetization than that of lignin-coated Fe_3O_4 (Figure 6). The results were confirmed through a magnetization vs. temperature profile in a 0.1 T externally applied magnetic field (Figure 7). Although the pure Fe_3O_4 nanoparticles do have a slightly higher magnetization than lignin-coated Fe_3O_4 above ~200 K, no substantial differences in the magnetization measurements were observed at any temperatures. This result confirms that lignin presence and encapsulation at the surface of the Fe_3O_4 nanoparticles does not significantly affect the nanocomposite magnetic properties using a 3:1 mass ratio of lignin to Fe_3O_4 in the preparation of the lignin magnetic nanocomposites. We have demonstrated the effect of increasing the lignin to magnetite ratio in a separate study, and similar results were obtained [35]. Magnetization increased linearly with temperature up to 100 K for both lignin@Fe_3O_4 and pure Fe_3O_4 and remained almost constant above 200 K, with a value of ~53 emu/g for both uncoated Fe_3O_4 and lignin@Fe_3O_4.

Additional characterization analysis of the lignin@Fe_3O_4 prepared using a 3:1 mass ratio of lignin to Fe_3O_4 and uncoated Fe_3O_4 nanomaterials can be found in the Supplemental Materials (Sections S1 and S2). These analyses include FT-IR and XRD. FT-IR validated the lignin presence on the Fe_3O_4 cores, and XRD confirmed Fe_3O_4 as the iron oxide nanoparticle structure.

3.3. Thermal Conductivity Measurements of Lignin@Fe_3O_4 and Fe_3O_4 Aqueous Agar Suspensions

Thermal conductivity for the nanomaterial colloidal suspensions increased with increasing concentrations and temperatures, as shown in Figure 8. For the lowest lignin@Fe_3O_4 concentration analyzed, around 0.001% w/v, there was no noticeable change in thermal conductivity compared to the aqueous agar suspension. However, as the concentration increased, a noticeable increase in thermal conductivity of 10% was observed when adding 0.005% w/v of lignin@Fe_3O_4 and raising the temperature to 45 °C. This thermal conductivity boost is possibly due to the interaction between nanoparticles and Brownian motion. The short distance between the particles increases interparticle and particle–fluid interactions in more concentrated suspensions. The collision between the nanoparticles due to Brownian motion and the thermal interaction of dynamic nanoparticles with the carrier fluid molecules increases [37]. The vigorous and relentless interactions between the liquid

molecules and nanoparticles at the molecular and nanoscale levels translate the energy into conduction at the macroscopic level due to the absence of bulk flow [37]. Additionally, at higher temperatures, the carrier fluid's viscosity is decreased, resulting in greater Brownian motion of nanoparticles, ultimately generating convection-like effects that remarkably increase conductivities. These motions and collision between the base fluid molecule carry the energy and travel in a mean-free pathway, increasing the thermal conductivity of the base fluid. Increasing the temperature and concentration not only increases the particle Brownian motion and interaction between the nanoparticles and molecules of the base fluid and facilitates the energy transfer mechanism but also increases the critical heat flux and substantial increment of the heat transfer coefficient that results in the enhancement of thermal conductivity [38]. This study, however, uses agar-based aqueous solutions as the base fluid and seeks to discover if significant thermal conductivity changes are also observed. For all trials, the thermal conductivity of base fluid was boosted by only 10% with the addition of 0.005% w/v lignin@Fe_3O_4 nanoparticles at 45 °C. This concludes that lignin@Fe_3O_4 nanoparticles increase the thermal conductivity of conventional heat transfer fluids, including agar-based aqueous solutions.
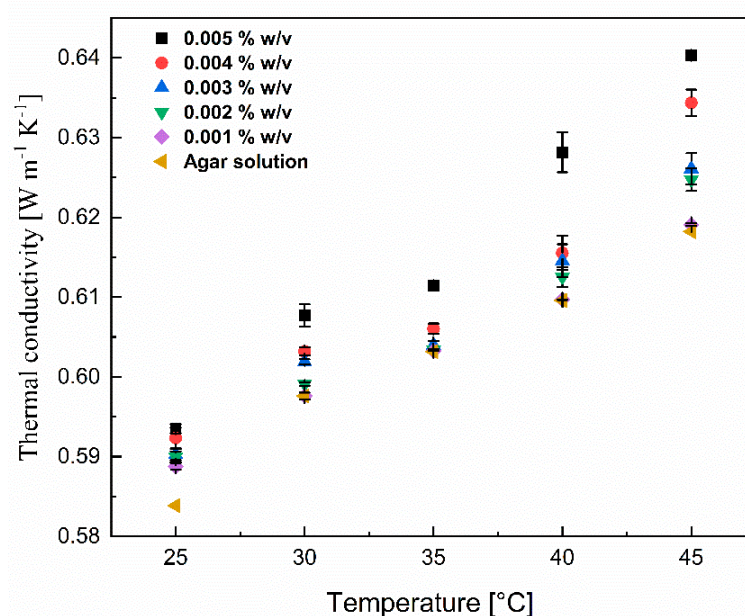

Figure 8. Thermal conductivity of lignin@Fe_3O_4 nanoparticles at various concentrations (0.001% w/v to 0.005% w/v) dispersed in a 0.1% w/v of agar aqueous suspensions at various temperatures and concentrations.

To compare the lignin coating effect on the thermal conductivity of the Fe_3O_4 nanosuspension, the thermal conductivity of pure Fe_3O_4 nanoparticles was also measured and the results are shown in Figure 9. Similar to the effect of lignin@Fe_3O_4 nanoparticles dispersed in agar-based aqueous suspensions, the thermal conductivity of suspensions containing only an Fe_3O_4 nanoparticle increased with increasing concentration and temperature. Note, however, the enhancement of thermal conductivity of lignin@Fe_3O_4 was around 3% higher than the uncoated Fe_3O_4 nanoparticles, slightly larger at higher concentrations. This increase in the thermal conductivity results is possibly due to the increased colloidal stability of the lignin-modified Fe_3O_4 in the suspension, leading to less aggregated nanostructures within the agar-based aqueous solution. This study used pH-induced precipitation to prepare hydrophobic lignin-based magnetic nanoparticles. Such a chemical modification method reduces its hydrophilicity and enhances the hydrophobic nature of lignin-based magnetic nanoparticles, which ultimately increases the dispersion rate and stability [18,39,40] and, therefore, the thermal conductivity. In addition, as shown in the

TEM images, the lignin encapsulation helped in particle size dispersion, which significantly enhanced the thermal conductivity [39].
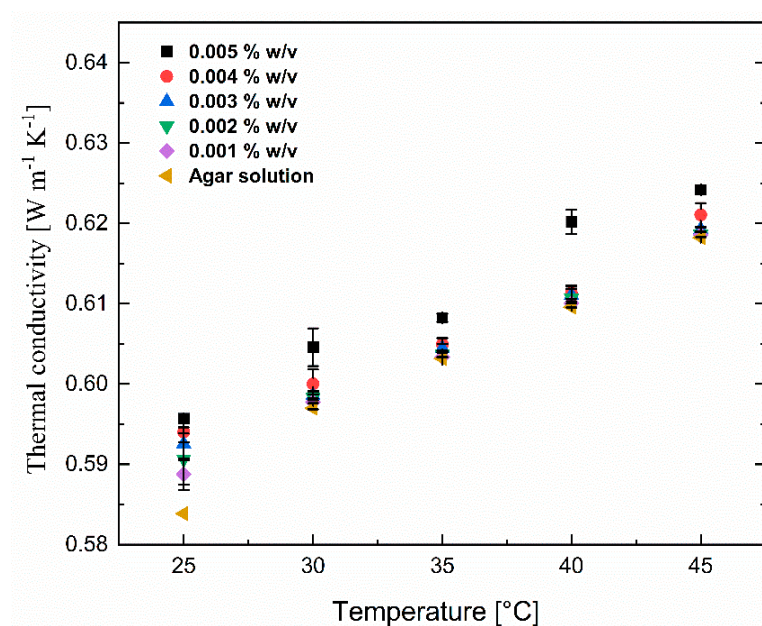

Figure 9. Thermal conductivity of pure Fe_3O_4 nanoparticles at various concentrations (0.001% *w/v* to 0.005% *w/v*) dispersed in 0.1% *w/v* agar aqueous suspensions at various temperatures and concentrations.

The thermal conductivities of various lignin@Fe_3O_4 colloidal nanosuspensions at different magnetic fields at room temperature are shown in Figure 10. With increasing magnetic field strength up to 0.02 T, the thermal conductivity was improved; however, the enhancement decreased drastically with further magnetic field strength increases. This peak maximum thermal conductivity has been reported for ferrofluids containing carbon nanotubes [41]. It is, however, the first time that this is reported for coated magnetic nanoparticles dispersed in an agar-based aqueous solution. The alignment of magnetic nanoparticles, which alters the thermophysical properties of magnetic nanofluids, in the direction of the magnetic field was responsible for the improvement of the suspension's thermal conductivity [28,41–43]. As the magnetic field increases, the magnetization of the nanoparticles generates an attraction force stronger than the electrostatic attraction; this, in conjunction with the alignment of the magnetic dipoles, induces the formation of a chain-like structure [11,28,42,43]. The length of chains increases with increased magnetic field until the path length of the sample cell [44]. These clusters are believed to enhance the thermal conductivity of lignin@Fe_3O_4 nanoparticles by up to 5% compared with its base fluid. With increment fields greater than 0.02 T, the nanoparticles likely feel force strong enough to move them towards the external magnet [28]. As the nanoparticles move to the vessel's wall [11], the thermal conductivity decreases due to the lower concentration of nanoparticles dispersed in the fluid. Figure 11 shows similar results for the case of pure Fe_3O_4 nanoparticles; in this case, the conductivity increment, of 5%, induced by the magnetic field was just slightly lower than that caused by the lignin@Fe_3O_4 nanocomposite. In both cases, the enhancement is due to the aggregation effect and alignment of the nanoparticles [45,46].
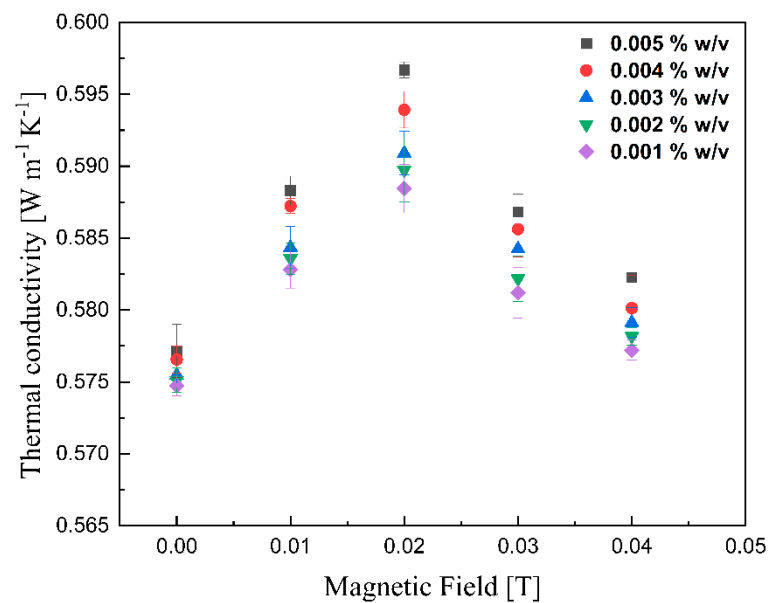
Figure 10. Measurement of thermal conductivity of lignin@Fe_3O_4 colloidal nanosuspension as a function of the magnetic field.
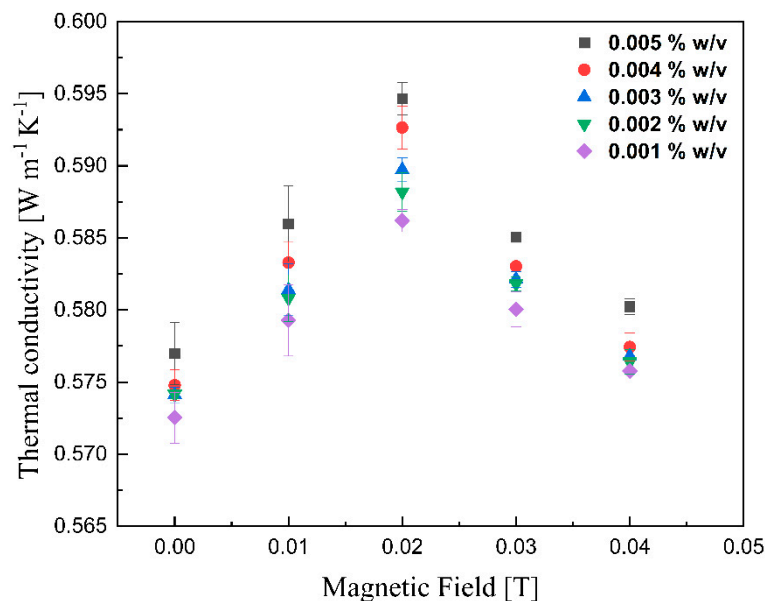

Figure 11. Measurement of thermal conductivity of pure Fe_3O_4 colloidal nanosuspension as a function of the magnetic field.

4. Conclusions

A 10% maximum thermal conductivity enhancement was achieved after adding lignin@Fe_3O_4 nanocomposites and pure Fe_3O_4 nanoparticles (0.005% *w/v*) in agar aqueous solutions at 45 °C. The thermal conductivity was improved as a function of concentration and temperature. Applying a magnetic field using a permanent magnet on the colloidal suspension with a magnetic field up to 0.02 T led to a maximum peak increase in each suspension's thermal conductivity, followed by a thermal conductivity decrease at higher magnetic fields for the uncoated and lignin-coated magnetic nanoparticle suspensions, respectively. The enhancement in thermal conductivity is attributed exclusively to magnetic nanoparticles. The decrease in thermal conductivity at higher magnetic fields is attributed to potential aggregate formation for both types of particles within the agar solution. Neg-

ligible differences, ~0.5%, were observed for the thermal conductivity of lignin@Fe_3O_4 compared with pure Fe_3O_4 for the same concentration and magnetic field strength. This slight difference in the thermal conductivity is attributed to the surface characteristics and magnetic behavior of the Fe_3O_4 and lignin-coated Fe_3O_4 nanoparticles.

Supplementary Materials: The following supporting information can be downloaded at: https://www.mdpi.com/article/10.3390/magnetochemistry10020012/s1, Figure S1: Thermal conductivity measurements of lignin@Fe_3O_4 agar-based aqueous suspensions at room temperature using a permanent magnet; Table S1: Magnetic field strengths as a function of distance for the permanent magnet. Section S1. Detailed procedure for the synthesis of lignin@Fe_3O_4 nanoparticles [47]; Figure S2. Experimental apparatus used for the synthesis of lignin@Fe_3O_4 nanoparticles; Section S2. FT-IR Analysis; Figure S3. FT-IR spectra of lignin, Fe_3O_4 and lignin@Fe_3O_4.; Section S3. X-ray diffraction (XRD) analysis; Figure S4: XRD spectra of neat lignin, pure Fe_3O_4, and 3:1 ratio of lignin@Fe_3O_4 nanoparticles. Six peaks at $30°$, $35°$, $43°$, $53°$, $57°$, and $63°$ correspond to the miller indices of 220, 311, 400, 422, 511, and 440, respectively, indicating particles have face-center cubic lattice structure [48,49].

References

1. Abu-Nada, E. Effects of variable viscosity and thermal conductivity of Al_2O_3–water nanofluid on heat transfer enhancement in natural convection. *Int. J. Heat Fluid Flow* **2009**, *30*, 679–690. [CrossRef]
2. Choi, S.U.S.; Eastman, J.A. *Enhancing Thermal Conductivity of Fluids with Nanoparticles*; No. ANL/MSD/CP-84938; CONF-951135-29: Argonne National Lab. (ANL): Argonne, IL, USA, 1995.
3. Puliti, G.; Paolucci, S.; Sen, M. Nanofluids and their properties. *Appl. Mech. Rev.* **2011**, *64*, 30803. [CrossRef]
4. Sangaiya, P.; Jayaprakash, R. A review on iron oxide nanoparticles and their biomedical applications. *J. Supercond. Nov. Magn.* **2018**, *31*, 3397–3413. [CrossRef]
5. Arico, A.S.; Bruce, P.; Scrosati, B.; Tarascon, J.M.; Van Schalkwijk, W. Nanostructured materials for advanced energy conversion and storage devices. *Nat. Mater.* **2005**, *4*, 366–377. [CrossRef] [PubMed]
6. Younes, H.; Mao, M.; Murshed, S.S.; Lou, D.; Hong, H.; Peterson, G. Nanofluids: Key parameters to enhance thermal conductivity and its applications. *Appl. Therm. Eng.* **2022**, *207*, 118202. [CrossRef]
7. Maxwell, J.C. *A Treatise on Electricity and Magnetism*; Clarendon Press: Oxford, UK, 1873; Volume 1.
8. Gui, N.G.J.; Stanley, C.; Nguyen, N.-T.; Rosengarten, G. Ferrofluids for heat transfer enhancement under an external magnetic field. *Int. J. Heat Mass Transf.* **2018**, *123*, 110–121. [CrossRef]
9. Taylor, R.; Coulombe, S.; Otanicar, T.; Phelan, P.; Gunawan, A.; Lv, W.; Rosengarten, G.; Prasher, R.; Tyagi, H. Small particles, big impacts: A review of the diverse applications of nanofluids. *J. Appl. Phys.* **2013**, *113*, 011301. [CrossRef]

10. Kleinstreuer, C.; Feng, Y. Experimental and theoretical studies of nanofluid thermal conductivity enhancement: A review. *Nanoscale Res. Lett.* **2011**, *6*, 1–13.
11. Lajvard, M.; Moghimi-Rad, J.; Hadi, I.; Gavili, A.; Isfahani, T.D.; Zabihi, F.; Sabbaghzadeh, J. Experimental investigation for enhanced ferrofluid heat transfer under magnetic field effect. *J. Magn. Magn. Mater.* **2010**, *322*, 3508–3513. [CrossRef]
12. Hasan, M.J.; Chen, P.; Dominick, N.; Vasquez, E.S.; Ureña-Benavides, E.E. Novel castor oil/water/ethanol Pickering emulsions stabilized by magnetic nanoparticles and magnetically controllable demulsification. *Colloids Surf. A.* **2023**, *677 Pt B*, 132424. [CrossRef]
13. Popescu, R.C.; Andronescu, E.; Vasile, B.S. Recent advances in magnetite nanoparticle functionalization for nanomedicine. *Nanomaterials* **2019**, *9*, 1791. [CrossRef]
14. Daoush, W.M. Co-precipitation and magnetic properties of magnetite nanoparticles for potential biomedical applications. *J. Nanomed. Res.* **2017**, *5*, 118. [CrossRef]
15. Woo, K.; Hong, J.; Choi, S.; Lee, H.-W.; Ahn, J.-P.; Kim, C.S.; Lee, S.W. Easy synthesis and magnetic properties of iron oxide nanoparticles. *Chem. Mater.* **2004**, *16*, 2814–2818. [CrossRef]
16. Sadeghinezhad, E.; Mehrali, M.; Saidur, R.; Mehrali, M.; Latibari, S.T.; Akhiani, A.R.; Metselaar, H.S.C. A comprehensive review on graphene nanofluids: Recent research, development and applications. *Energy Convers. Manag.* **2016**, *111*, 466–487. [CrossRef]
17. Leong, K.; Ahmad, K.K.; Ong, H.C.; Ghazali, M.; Baharum, A. Synthesis and thermal conductivity characteristic of hybrid nanofluids—A review. *Renew. Sustain. Energy Rev.* **2017**, *75*, 868–878. [CrossRef]
18. Schneider, W.D.H.; Dillon, A.J.P.; Camassola, M. Lignin nanoparticles enter the scene: A promising versatile green tool for multiple applications. *Biotechnol. Adv.* **2021**, *47*, 107685. [CrossRef] [PubMed]
19. Xiao, D.; Ding, W.; Zhang, J.; Ge, Y.; Wu, Z.; Li, Z. Fabrication of a versatile lignin-based nano-trap for heavy metal ion capture and bacterial inhibition. *Chem. Eng. J.* **2019**, *358*, 310–320. [CrossRef]
20. Kai, D.; Tan, M.J.; Chee, P.L.; Chua, Y.K.; Yap, Y.L.; Loh, X.J. Towards lignin-based functional materials in a sustainable world. *Green Chem.* **2016**, *18*, 1175–1200. [CrossRef]
21. Zhou, X.; Jin, C.; Liu, G.; Wu, G.; Huo, S.; Kong, Z. Functionalized lignin-based magnetic adsorbents with tunable structure for the efficient and selective removal of Pb(II) from aqueous solution. *Chem. Eng. J.* **2021**, *420*, 130409. [CrossRef]
22. Ebrahimi, R.; de Faoite, D.; Finn, D.; Stanton, K. Accurate measurement of nanofluid thermal conductivity by use of a polysaccharide stabilising agent. *Int. J. Heat Mass Transf.* **2019**, *136*, 486–500. [CrossRef]
23. Abareshi, M.; Goharshadi, E.K.; Zebarjad, S.M.; Fadafan, H.K.; Youssefi, A. Fabrication, characterization and measurement of thermal conductivity of Fe_3O_4 nanofluids. *J. Magn. Magn. Mater.* **2010**, *322*, 3895–3901. [CrossRef]
24. Rajan, A.; Sharma, M.; Sahu, N.K. Assessing magnetic and inductive thermal properties of various surfactants functionalised Fe_3O_4 nanoparticles for hyperthermia. *Sci. Rep.* **2020**, *10*, 15045. [CrossRef]
25. Cakmak, N.K.; Said, Z.; Sundar, L.S.; Ali, Z.M.; Tiwari, A.K. Preparation, characterization, stability, and thermal conductivity of rGO-Fe_3O_4-TiO_2 hybrid nanofluid: An experimental study. *Powder Technol.* **2020**, *372*, 235–245. [CrossRef]
26. Ma, H.; Gao, B.; Wang, M.; Yuan, Z.; Shen, J.; Zhao, J.; Feng, Y. Strategies for enhancing thermal conductivity of polymer-based thermal interface materials: A review. *J. Mater. Sci.* **2021**, *56*, 1064–1086. [CrossRef]
27. Kugabaeva, G.D.; Kydralieva, K.A.; Bondarenko, L.S.; Baimuratova, R.K.; Karpenkov, D.Y.; Golovkova, E.A.; Degtyarenko, P.N.; Golubeva, N.D.; Uflyand, I.E.; Dzhardimalieva, G.I. Polymer-Assisted Synthesis, Structure and Magnetic Properties of Bimetallic FeCo-and FeNi/N-Doped Carbon Nanocomposites. *Magnetochemistry* **2023**, *9*, 213. [CrossRef]
28. Doganay, S.; Turgut, A.; Cetin, L. Magnetic field dependent thermal conductivity measurements of magnetic nanofluids by 3ω method. *J. Magn. Magn. Mater.* **2019**, *474*, 199–206. [CrossRef]
29. Tlili, H.; Elaoud, A.; Asses, N.; Horchani-Naifer, K.; Ferhi, M.; Goya, G.F.; Fuentes-García, J.A. Reduction of Oxidizable Pollutants in Waste Water from the Wadi El Bey River Basin Using Magnetic Nanoparticles as Removal Agents. *Magnetochemistry* **2023**, *9*, 157. [CrossRef]
30. Massart, R. Preparation of aqueous magnetic liquids in alkaline and acidic media. *IEEE Trans. Magn.* **1981**, *17*, 1247–1248. [CrossRef]
31. Petrie, F.A. Magnetic-Lignin Nanoparticles as Potential Ethanol Extractants from Aqueous Solutions. M.S. Thesis, University of Dayton, Dayton, OH, USA, 2019.
32. Westphal, E.N. Lignin-Magnetite Nanoparticles Aiding in Pickering Emulsions and Oil Manipulation and Their Rheological Properties. Master's Thesis, University of Dayton, Dayton, OH, USA, 2021.
33. Hasan, M.J.; Westphal, E.; Chen, P.; Saini, A.; Chu, I.-W.; Watzman, S.J.; Ureña-Benavides, E.; Vasquez, E.S. Adsorptive properties and on-demand magnetic response of lignin@Fe_3O_4 nanoparticles at castor oil–water interfaces. *RSC Adv.* **2023**, *13*, 2768–2779. [CrossRef] [PubMed]
34. Hasan, M.J.; Yeganeh, F.; Ciric, A.; Chen, P.; Vasquez, E.S.; Ureña-Benavides, E.E. Liquid-Liquid Equilibria of Water+ Ethanol+ Castor Oil and the Effect of Cellulose Nanocrystal/Fe_3O_4 and Lignin/Fe_3O_4 Nanoparticles. *J. Chem. Thermodyn.* **2023**, *180*, 107007. [CrossRef]
35. Petrie, F.A.; Gorham, J.M.; Busch, R.T.; Leontsev, S.O.; Ureña-Benavides, E.E.; Vasquez, E.S. Facile fabrication and characterization of kraft lignin@Fe_3O_4 nanocomposites using pH driven precipitation: Effects on increasing lignin content. *Int. J. Biol. Macromol.* **2021**, *181*, 313–321. [CrossRef]

36. Wang, Y.-Y.; Meng, X.; Pu, Y.; Ragauskas, A.J. Recent Advances in the Application of Functionalized Lignin in Value-Added Polymeric Materials. *Polymers* **2020**, *12*, 2277. [CrossRef]

37. Jang, S.P.; Choi, S.U.S. Role of Brownian motion in the enhanced thermal conductivity of nanofluids. *Appl. Phys. Lett.* **2004**, *84*, 4316–4318. [CrossRef]

38. Kang, H.U.; Kim, S.H.; Oh, J.M. Estimation of thermal conductivity of nanofluid using experimental effective particle volume. *Exp. Heat Transf.* **2006**, *19*, 181–191. [CrossRef]

39. Shorey, R.; Gupta, A.; Mekonnen, T.H. Hydrophobic modification of lignin for rubber composites. *Ind. Crop. Prod.* **2021**, *174*, 114189. [CrossRef]

40. Wang, H.; Yang, D.; Xiong, W.; Liu, W.; Qiu, X. One-pot preparation of hydrophobic lignin/SiO_2 nanoparticles and its reinforcing effect on HDPE. *Int. J. Biol. Macromol.* **2021**, *180*, 523–532. [CrossRef]

41. Shahsavar, A.; Salimpour, M.R.; Saghafian, M.; Shafii, M.B. Effect of magnetic field on thermal conductivity and viscosity of a magnetic nanofluid loaded with carbon nanotubes. *J. Mech. Sci. Technol.* **2016**, *30*, 809–815. [CrossRef]

42. Nkurikiyimfura, I.; Wang, Y.; Pan, Z. Heat transfer enhancement by magnetic nanofluids—A review. *Renew. Sustain. Energy Rev.* **2013**, *21*, 548–561. [CrossRef]

43. Bahiraei, M.; Hangi, M. Flow and heat transfer characteristics of magnetic nanofluids: A review. *J. Magn. Magn. Mater.* **2015**, *374*, 125–138. [CrossRef]

44. Philip, J.; Shima, P.D.; Raj, B. Enhancement of thermal conductivity in magnetite based nanofluid due to chainlike structures. *Appl. Phys. Lett.* **2007**, *91*, 203108. [CrossRef]

45. Wang, B.; Monroe, J.G.; Kumari, S.; Leontsev, S.O.; Vasquez, E.S.; Thompson, S.M.; Berg, M.J.; Walters, D.K.; Walters, K.B. Analytical model for electromagnetic induction in pulsating pipe flows. *Int. J. Heat Mass Transf.* **2021**, *175*, 121325. [CrossRef]

46. Vasquez, E.S.; Prehn, E.M.; Walters, K.B. Assessing magnetic iron oxide nanoparticle properties under different thermal treatments. *J. Therm. Anal. Calorim.* **2021**, *143*, 35–46. [CrossRef]

47. Priyadarshana, G.; Kottegoda, N.; Senaratne, A.; Alwis, A.D.; Karunaratne, V. Synthesis of magnetite nanoparticles by top-down approach from a high purity ore. *J. Nanomater.* **2016**, *16*, 317. [CrossRef]

48. Mirzazadeh Ghanadi, A.; Heydari Nasab, A.; Bastani, D.; Seife Kordi, A.A. The effect of nanoparticles on the mass transfer in liquid–liquid extraction. *Chem. Eng. Commun.* **2015**, *202*, 600–605. [CrossRef]

49. Ounacer, M.; Essoumhi, A.; Sajieddine, M.; Razouk, A.; Costa, B.F.O.; Dubiel, S.M.; Sahlaoui, M. Structural and magnetic studies of annealed iron oxide nanoparticles. *J. Supercond. Nov. Magn.* **2020**, *33*, 3249–3261. [CrossRef]

50. Gautam, B. Tuning the Thermal Conductivity of Lignin@Fe_3O_4 Colloidal Suspension through External Magnetic Field. Master's Thesis, University of Dayton, Dayton, OH, USA, 2022. Available online: http://rave.ohiolink.edu/etdc/view?acc_num=dayton1671034996620314 (accessed on 1 February 2024).